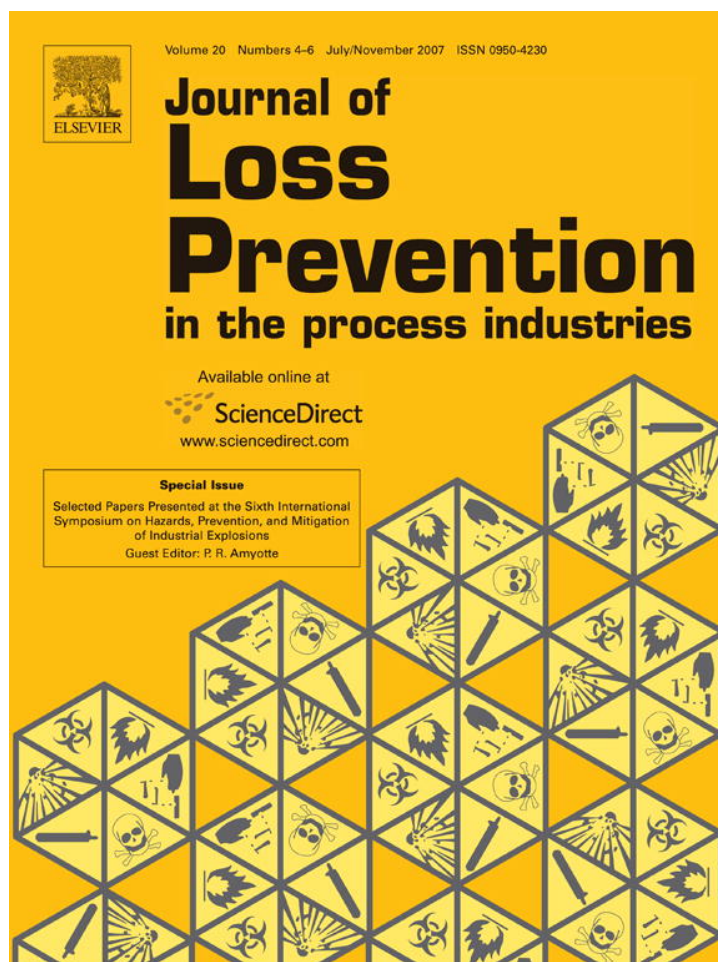


Provided for non-commercial research and education use.  
Not for reproduction, distribution or commercial use.



This article was published in an Elsevier journal. The attached copy is furnished to the author for non-commercial research and education use, including for instruction at the author's institution, sharing with colleagues and providing to institution administration.

Other uses, including reproduction and distribution, or selling or licensing copies, or posting to personal, institutional or third party websites are prohibited.

In most cases authors are permitted to post their version of the article (e.g. in Word or Tex form) to their personal website or institutional repository. Authors requiring further information regarding Elsevier's archiving and manuscript policies are encouraged to visit:

<http://www.elsevier.com/copyright>



# Reactive shock and detonation propagation in U-bend tubes

S.M. Frolov\*, V.S. Aksenov, I.O. Shamshin

*Semenov Institute of Chemical Physics, 4, Kosigin Street, Moscow 119991, Russia*

Received 26 November 2006; received in revised form 10 March 2007; accepted 11 March 2007

---

## Abstract

The objective of the research outlined in this paper was to provide new experimental and computational data on initiation, propagation, and stability of gaseous stoichiometric propane–air detonations in tubes with U-bends. Extensive experimental and computational studies with the tube 51 mm in diameter with U-bends of two curvatures and two different shock-wave generators were performed. Numerical simulations of the process were used to reveal the salient features of the accompanying phenomena.

© 2007 Elsevier Ltd. All rights reserved.

*Keywords:* Gaseous detonation; Shock-to-detonation transition; Tube with U-bends

---

## 1. Introduction

Tube bends and coils are the elements, which are widely used in various industrial applications. Surprisingly, little work has been done on the reactive shock and detonation diffraction in such elements (Frolov, Aksenov, & Basevich, 2005; Frolov, Aksenov, & Shamshin, 2005, 2007; Frolov, Basevich, & Aksenov, 2004, 2005a,b; Nettleton, 1987), although the phenomenon of focusing of shock waves in straight tubes after reflection from a nonflat end wall has long been known (Sturtevant & Kulkarny, 1976). Our recent research on deflagration-to-detonation transition (DDT) and shock-to-detonation transition (SDT) in curved tubes (Frolov, Aksenov, & Basevich, 2005; Frolov, Aksenov, & Shamshin, 2005, 2007; Frolov, Basevich, & Aksenov, 2004, 2005a,b) has unequivocally demonstrated that tube curvature promoted DDT and SDT efficiently.

Frolov, Aksenov, and Basevich (2005), and Frolov, Basevich, and Aksenov (2004, 2005a,b) studied the effect of tube coils on DDT and direct detonation initiation in homogeneous and two-phase reactive media. The use of smooth-walled tubes with coils allowed decreasing the critical energy of direct detonation initiation at least by a factor of two. As for the DDT in the straight tube with the

Shchelkin spiral followed by the tube coil, it was solely attributed to the use of the tube coil.

In Frolov, Aksenov, and Shamshin (2005, 2007), the experimental and computational results were reported for the SDT in a stoichiometric propane–air mixture in a tube with a single U-bend of the internal radius equal to tube diameter (51 mm). The results demonstrated a considerable effect of the U-bend on detonation initiation and propagation. On the one hand, the U-bend of the tube promoted the SDT: a shock wave entering the U-bend at a velocity exceeding 1100 m/s always transitioned to a detonation. On the other hand, the detonation wave propagating at a velocity of 1700–1800 m/s through the U-bend was subjected to temporary attenuation with the velocity drop of about 250 m/s (15%) followed by the recovery of the propagation velocity in the straight tube section downstream from the U-bend. Two-dimensional numerical simulations of detonation transition through the U-bend revealed salient features of transient phenomena in U-tubes. It was shown that different portions of the lead detonation front exhibited different behavior in the U-bend due to temporally and spatially shifted interaction with various compression and rarefaction waves and due to finite rate of chemical reaction. Both localized detonation decay and detonation reinitiation events were detected near the internal wall of the U-bend. In addition, large-scale unburned fuel pockets far behind the lead shock front were

---

\*Corresponding author. Tel.: +7 095 9397228.

E-mail address: [smfrol@chph.ras.ru](mailto:smfrol@chph.ras.ru) (S.M. Frolov).

shown to form during detonation transition through the U-bend. After exiting from the U-bend, the detonation recovered at a distance of about 8–10 tube diameters attaining an established cellular structure.

The curvature of the U-bend, tube diameter, and compression phase duration of the initiating shock wave are expected to be the most important governing parameters of the problem which determine the evolution of the initiating shock wave or a developed detonation wave in such a system (Frolov et al., 2007). The objective of the research outlined in this paper was to provide new experimental and computational data on propagation of reactive shock and detonation waves in tubes with U-bends. The research is mainly focused on the effect of U-tube curvature and compression-phase duration of the incident shock wave on SDT.

## 2. Experimental setups

The experimental setups used in this study are shown in Figs. 1–3. All the setups comprised the detonation tube of round cross-section with two U-bends. The tube was fixed at the experimental stand, which was equipped with the utilities required for working with gaseous explosive mixtures. The explosive mixture was the stoichiometric propane–air. The mixture was prepared in the mixer at normal atmospheric conditions. The theoretical Chapman–Jouguet detonation velocity of the mixture is 1804 m/s. At one end of the tube, a shock generator (SG) was mounted. Two types of SG were used: solid-propellant SG (Fig. 1) and electric-discharge SG (Figs. 2 and 3).

The solid-propellant SG was a combustion chamber of 22 cm<sup>3</sup> in volume equipped with a changeable nozzle of up to 14 mm in diameter closed with a bursting diaphragm. Before the run the combustion chamber was filled with a solid propellant with a mass of up to 2.5 g. The propellant was ignited by an igniter 0.2 ± 0.02 g in mass. The maximal pressure in the chamber was up to 100 MPa. The strength of the shock wave formed depended on the nozzle diameter, diaphragm thickness, and thermodynamic parameters of combustion products in the SG.

The electric-discharge SG was the same as used earlier by Frolov, Aksenov, and Basevich (2005), Frolov, Aksenov, and Shamshin (2005, 2007) and Frolov, Basevich, and Aksenov (2004, 2005a,b) and comprised three electrodes. The distance between two main electrodes was 8 mm. The primary (breakdown) discharge gap was 3 mm. The primary discharge was of fixed (57 J) energy. It produced plasma to trigger the main discharge of considerably higher energy. Capacitance of main discharge was 800 μF. The voltage varied from 1.5 to 2.5 kV. The characteristic time of discharge was 20–40 μs.

The tube 51 mm in inner diameter had three straight sections and two U-bends, both in one plane. The internal radius of the U-bends was 11 mm while the axial radius was 37 mm. Each U-bend was fabricated by welding four curved segments. Up to 10 piezoelectric pressure transducers (D1–D10) were mounted along the tube axis (see Figs. 1–3 and Tables 1–3). In the setups of Figs. 1 and 2, the lengths of the straight tube sections were 1005–1200 mm each and the

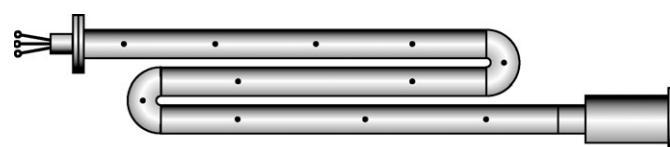


Fig. 2. Experimental setup with the electric-discharge SG. Dots indicate the positions of pressure transducers (see Table 2).

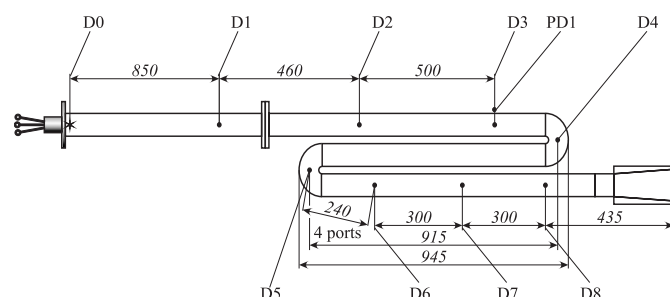


Fig. 3. Experimental setup with the electric-discharge SG and with the elongated initiation section. PD1 stands for photo-diode. Dots indicate the positions of pressure transducers (see Table 3).

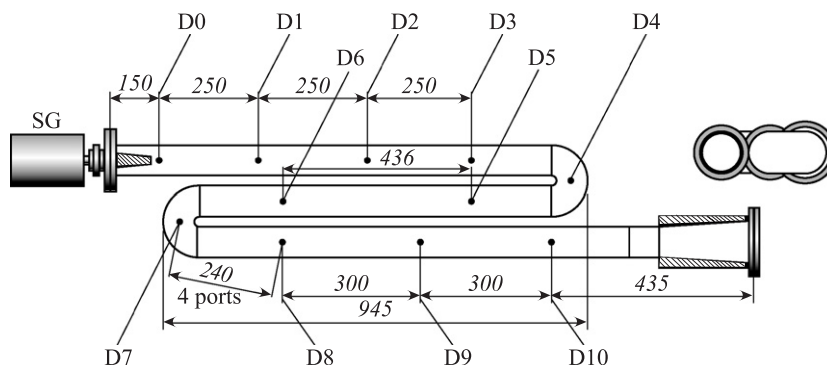


Fig. 1. Schematic of the experimental setup with the solid-propellant SG. Dimensions are in millimeters. Dots indicate the positions of pressure transducers (see Table 1).

Table 1  
Measuring ports in experiments with solid-propellant SG

No.	D1	D2	D3	D4	D5	D6	D7	D8	D9	D10
Distance (mm)	400	650	900	1140	1380	1816	2056	2296	2596	2896

Table 2  
Measuring ports in experiments with electric-discharge SG

No.	D1	D2	D3	D4	D5	D6	D7	D8	D9
Distance (mm)	650	900	1140	1380	1816	2056	2296	2596	2896

Table 3  
Measuring ports in experiments with electric-discharge SG and elongated tube

No.	D1	D2	D3	D4	D5	D6	D7	D8
Distance (mm)	850	1310	1810	2050	2726	2966	3206	3506

total length of the tube along the tube axis was 3330 mm. The setup of Fig. 3 had a straight-tube extension 850 mm long attached to the SG. The internal tube walls in all setups were smooth.

The accuracy of shock wave velocity measurements was estimated as 4%. The data acquisition system was triggered by pressure transducer D1. The measuring segments at the straight tube sections were 250 and 300 mm long. The measuring segments in the U-bends were 250 mm long when measured along the U-bend axis and 232 mm long when measured along the straight line connecting the neighboring measuring ports. For calculating the shock wave propagation velocity in the U-bends, the corresponding measuring segments were taken to be 240 mm long (the shortest distance between the neighboring measuring ports if measured inside the tube).

### 3. Experimental results

#### 3.1. Solid-propellant SG

The first experimental series was performed at the setup of Fig. 1. Fig. 4 shows the measured dependencies of the shock and detonation wave velocities on the distance traveled along the tube in some representative runs. Two vertical dashed lines show the positions of the U-bends. Shown in Fig. 4a is the variation of the mean shock velocity along the tube with two U-bends, when the solid-propellant SG generated an overdriven detonation at the first measuring segment (1800–2000 m/s) and the detonation wave transitioned through the U-bends. The detonation wave decelerated to 1510 m/s after the first U-bend, accelerated to 1660–1720 m/s in the intermediate straight tube section, decelerated again to 1430–1480 m/s after the second U-bend, and then recovered propagating at

1650–1800 m/s. The mean detonation velocity deficit in the regions behind the second U-bend attained the value of about 20%.

Fig. 4b shows the variation of the mean shock wave velocity along the tube, when the SG generated a shock wave with the velocity of 800–900 m/s at the first measuring segment. Due to attenuation in the straight section upstream the first U-bend, the shock waves entered the first U-bend at a mean velocity of 700–750 m/s in this experimental series. After passing the first U-bend, such shock waves propagated at a nearly constant velocity of 600–650 m/s along the intermediate straight tube section and decelerated to about 500 m/s after the second U-bend. There were indications of shock wave acceleration downstream the second U-bend up to 1100 m/s in some runs; however, the total length of the tube was insufficient for determining whether such waves were capable of transitioning to a detonation. For the sake of comparison, Fig. 4b shows the attenuation of a shock wave of initial velocity of 1300 m/s in pure air.

Fig. 4c shows the variation of the mean shock wave velocity along the tube with the initial shock wave velocities in the range from 850 to 1300 m/s at the first measuring segment. In this experimental series, the shock waves transitioned to detonations after passing either the first U-bend, or the second U-bend, i.e., the SDT phenomenon was detected. The lowest mean velocity of the primary shock wave entering the first U-bend and leading to the detonation onset behind the second U-bend was about 800 m/s. This velocity value should be treated as the critical condition for the setup of Fig. 1. Remind that in the experiments with a U-bend of smaller curvature (Frolov, Aksenov, & Shamshin, 2005), the critical shock wave velocity was about 1100 m/s. It is seen from Fig. 4c that the higher the primary shock velocity, the faster is the onset of detonation. However, in the vicinity of the critical velocity value, some hysteretic behavior of shock waves was observed. This kind of behavior is demonstrated in Fig. 4d.

Fig. 5 shows the pressure records relevant to some runs of Fig. 4. Remind that pressure transducers D4 and D7 are positioned in the first and the second U-bends. Detonation transition through the tube with two U-bends is shown in Fig. 5a.

Fig. 5b shows the pressure records relevant to the phenomena observed in the experimental series of Fig. 4b. Starting from the record of D4, one can see the formation of a strong secondary pressure wave in the wake of the primary shock wave. At the record of D9, the secondary shock wave has not yet caught up with the primary shock wave. Note that the third wave evident in Fig. 5b corresponds to the shock wave reflected from the closed end of the tube.

Pressure records in Fig. 5c and d correspond to the experimental series of Fig. 4c. In both cases, the formation of a secondary pressure wave is clearly seen at the record of D4. In Fig. 5c, the secondary explosion occurred somewhat

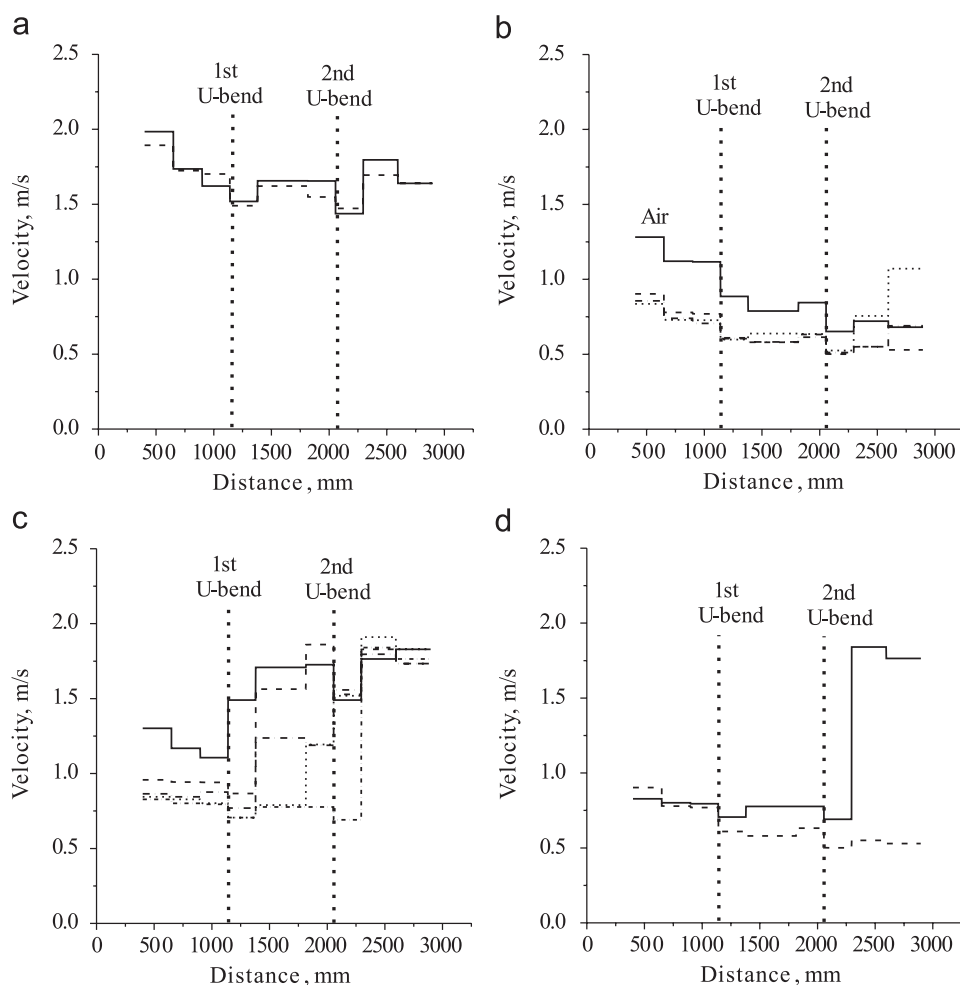


Fig. 4. Mean shock wave velocities at different measuring segments of the tube with two U-bends (shown by vertical lines) in some representative runs: (a) transition of detonation through two U-bends, (b) transition of shock waves through two U-bends without detonation onset, (c) transition of shock waves through two U-bends with detonation onset, and (d) phenomena in the vicinity of the critical primary shock intensity.

earlier than in Fig. 5d, and the detonation arose in the intermediate straight tube section between pressure transducers D4 and D7. In Fig. 5d, the detonation arose downstream the second U-bend. In both cases, the secondary shock wave caught up with the primary shock wave giving rise to a detonation.

### 3.2. Electric-discharge SG

The second experimental series was conducted at the setup of Fig. 2 with the electric-discharge SG. The main specific feature of this SG was that it generated the shock waves of shorter compression phase duration. Fig. 6 shows the measured dependencies of the shock and detonation wave velocities on the distance traveled along the tube in some representative runs. Again, the vertical dashed lines show the positions of the U-bends.

Similar to the experiments described in Section 3.1, the detonation wave, when passing through the U-bends, exhibited deep drops in the mean propagation velocity, but nevertheless recovered after the second U-bend.

Clearly, due to a short compression phase duration, the primary shock waves attenuated much stronger than in the setup of Fig. 1. For example, the primary shock wave with the mean velocity of about 1350 m/s at the first measuring segment attenuated to the velocity of about 800 m/s at the entrance to the first U-bend. A similar initial shock wave in the setup of Fig. 1 attenuated to about 1150 m/s. Nevertheless, the critical velocity value for the shock wave entering the first U-bend, required for detonation initiation, appeared to be also about 800 m/s, i.e. close to that found in Section 3.1.

Fig. 7 shows pressure records in two runs relevant to detonation transition through the U-bends (Fig. 7a) and SDT (Fig. 7b).

### 3.3. Electric-discharge SG with extension

The third experimental series was conducted at the setup of Fig. 3 with the electric-discharge SG and with the extension tube at the initiation side. The extension tube was used to vary the intensity of the primary shock wave at the

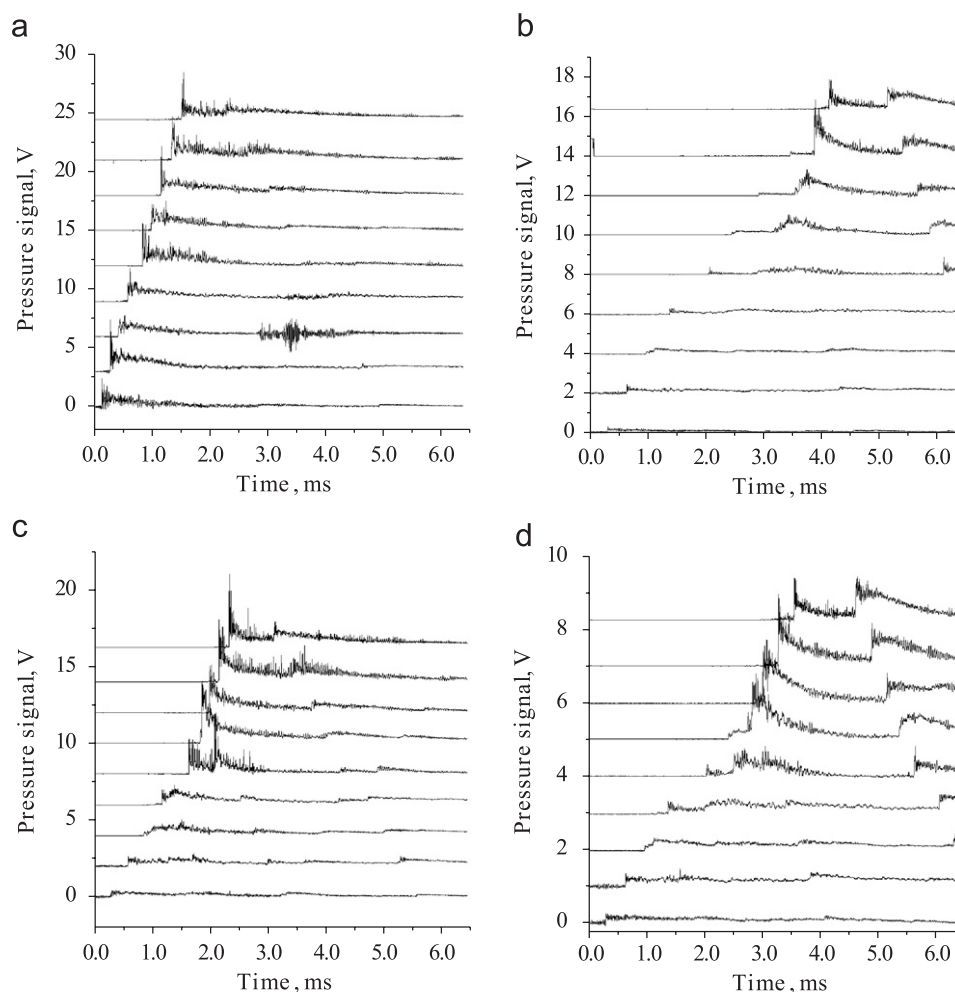


Fig. 5. Pressure records: (a) detonation, (b) shock wave with a strong pressure wave in the wake, (c) SDT, and (d) shock wave with the strong pressure wave catching up with the lead front.

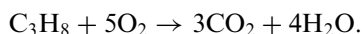
entrance to the first U-bend. Fig. 8 shows some measured dependencies of the shock and detonation wave velocities on the distance traveled along the tube. In this experimental series, the phenomenon of detonation decay in the U-bend was observed. One of the curves in Fig. 8 shows the event of detonation decay after it passes through the first U-bend. Due to the limited length of the tube in the setup of Fig. 3, it was not possible to judge whether the detonation was capable to recover or not after passing the second U-bend. The other important finding in this experimental series is that the critical velocity value for the shock wave entering the first U-bend to transition to detonation was also close to 800 m/s. One of the solid lines corresponds to the run with the shock wave entering the first U-bend at the mean velocity of 790 m/s, decaying to 440 m/s in the intermediate tube section, and accelerating up to 1340 m/s behind the second U-bend. Inspection of the corresponding pressure records made it possible to assume that the detonation would likely occur in the longer tube. For example, Fig. 9 shows the pressure records in the run relevant to detonation transition through the U-bends (Fig. 9a) and in the run relevant to possible SDT (Fig. 9b).

It follows from Fig. 9b that a strong secondary shock wave has nearly caught up with the decaying primary shock wave at pressure transducer D9 (upper record).

To be sure that the run in Fig. 9a dealt with the developed detonations, two techniques—photo-diode registration and smoked-foil footprints—were used for identifying the detonation. The record of photo-diode PD1 is shown in Fig. 9a. Remind, that in the setup of Fig. 3, the photo-diode was mounted in the same cross-section with the pressure transducer D3 and allowed identifying detonation or deflagration based on the time delay between shock wave arrival at pressure transducer D3 and flame front arrival at photo-diode PD1. In the records of Fig. 9a, the time delay between the signals was small (about 10  $\mu$ s) and therefore the primary shock wave was treated as a detonation wave. In the records of Fig. 9b, the time delay between shock wave and flame arrival at the position of D3 and PD1 was long (about 600  $\mu$ s) and therefore the primary shock wave was not treated as a detonation. The smoked foil technique was also used to identify detonation at the exit from the second U-bend.

#### 4. Computational analysis

The mathematical model was based on the standard two-dimensional Euler equations, energy conservation equation with a chemical source term, and equation of chemical kinetics. The kinetics of propane oxidation was modeled by a single-stage overall reaction



The heat effect of the reaction entering the energy conservation equation was taken equal to 46.6 MJ/kg. The expression for a bimolecular reaction rate  $w = k[\text{C}_3\text{H}_8][\text{O}_2]$  was used to calculate the rate of reaction, where  $k =$

$7 \times 10^{14} p^{-0.2264} \exp(-E/RT) \text{ cm}^3 \text{ mol}^{-1} \text{ s}^{-1}$  is the rate constant,  $T$  is the temperature,  $R$  is the gas constant,  $E = 45,460 \text{ kcal/mol}$  is the activation energy, and  $p$  is pressure in atm. The rate constant was obtained by fitting the calculated ignition delays with the experimental data on ignition of the stoichiometric propane–air mixture behind reflected shock waves (Frolov, Aksenov, & Shamshin, 2005). In the fitting calculations, a zero-dimensional, constant-volume exothermal reaction kinetics was considered. Two definitions of the ignition delay were used: (i) as a time corresponding to the maximal rate of temperature rise and (ii) as a time corresponding to the characteristic ignition temperature  $T = T_0 + RT_0^2/E$ , where  $T_0$  is the

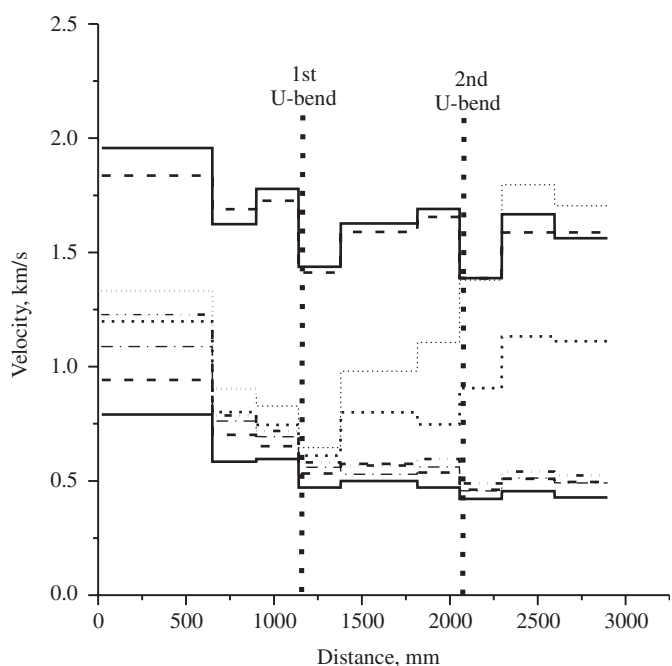


Fig. 6. Mean shock wave velocities at different measuring segments of the tube with two U-bends (shown by vertical lines) in some representative runs with electric-discharge SG.

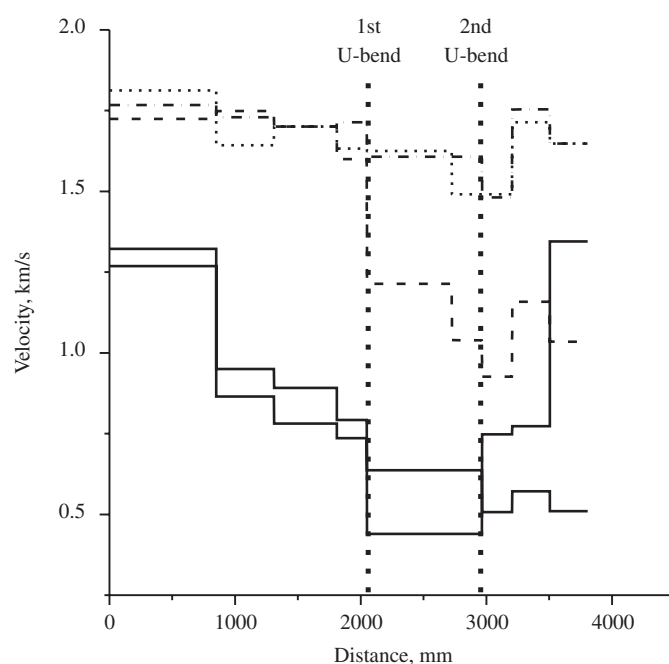


Fig. 8. Mean shock wave velocities at different measuring segments of the tube with two U-bends (shown by vertical lines) in representative runs.

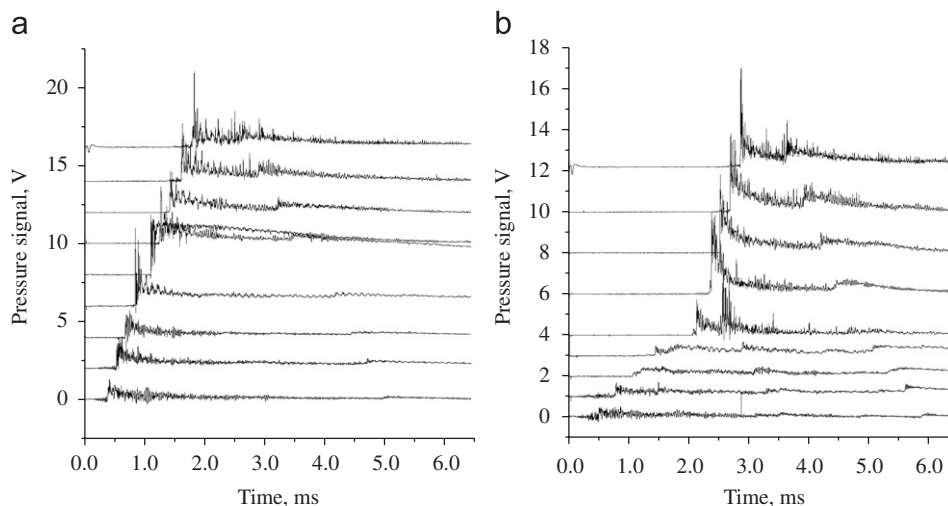


Fig. 7. Pressure records: (a) detonation; and (b) SDT.

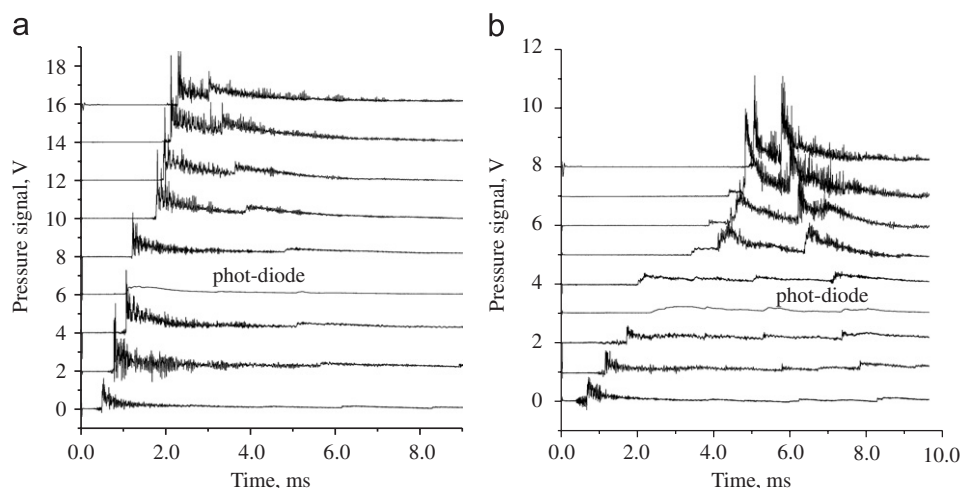


Fig. 9. Representative pressure records: (a) detonation with the photo-diode in the same cross-section with D3 and simultaneous signal; and (b) no shock-to-detonation transition with the time delay of photo-diode activation.

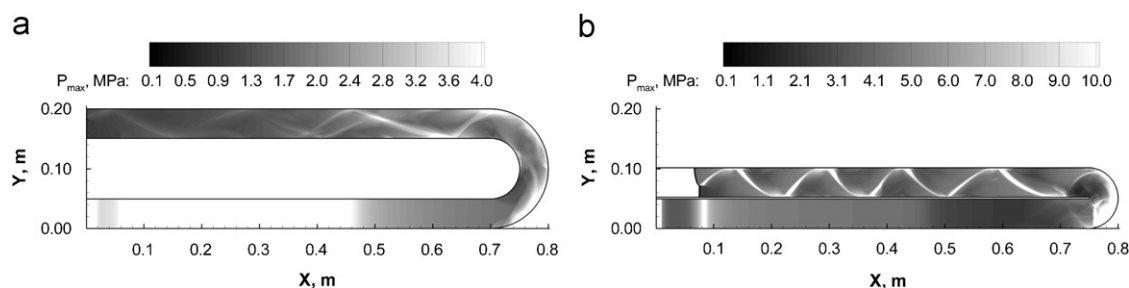


Fig. 10. Predicted fields of maximal pressure at identical conditions of shock wave generation in tubes with different U-bend curvature: (a) no detonation, and (b) detonation.

initial temperature. The resultant ignition delays obtained within both definitions were very close to each other.

For numerical solution of governing equations a method of splitting by physical processes was used. At each time step, only convective fluxes and pressure work were taken into account at the first stage. This stage of integration was solved by the second-order Godunov–Kolgan method. Mass, momentum, and energy fluxes through faces of a computational mesh were found from the exact solutions of the Riemann problem. At the second stage, the chemical reaction was taken into account. A fully implicit method was used for integrating the reaction kinetic equation. A more detailed description of the numerical procedure is available in Frolov, Aksenov, and Shamshin (2005).

Fig. 10 shows the comparison of calculations of SDT in a tube 51 mm in diameter with the U-bend of different curvature at identical initial conditions. Fig. 10a corresponds to the study of Frolov, Aksenov, and Shamshin (2005, 2007) with the U-bend curvature radius equal to the tube diameter. Fig. 10b corresponds to the tube with the U-bend studied herein. In both computational runs, the primary shock wave was generated by a high-pressure domain in a lower left end of the tube with a pressure of 18 MPa and temperature of 298 K. The resulting shock wave entering the U-bend had a velocity of about 1000 m/s.

It can be seen that a single-head detonation was initiated by such a shock wave in the tube with the U-bend of smaller curvature radius (Fig. 10b), while shock wave deceleration was detected in the tube with the U-bend of larger curvature radius (Fig. 10a). These results correspond well with the experimental findings.

The effect of compression phase duration in the primary shock wave is illustrated by Figs. 11a and b. In both cases, the primary shock wave velocity was 1460 m/s. The compression phase duration in the primary shock waves of Figs. 11a and b was 30 and 50  $\mu$ s, respectively. It is seen that the longer duration shock wave transitions first to a single-head detonation and then to a multihead detonation, i.e., exhibits SDT, whereas a shorter duration shock wave does not. Note that the secondary explosions occurring in the U-bend due to multiple shock reflections give also rise to a detonation propagating upstream, which manifests itself by a high-pressure region with fine cellular structure. The effect of compression phase duration in the primary shock on the SDT was studied computationally by Frolov et al. (2007) but has not been observed experimentally so far. Probably, the reason is that this parameter was not varied in a sufficiently wide range. In further experimental studies, this implication will be checked.

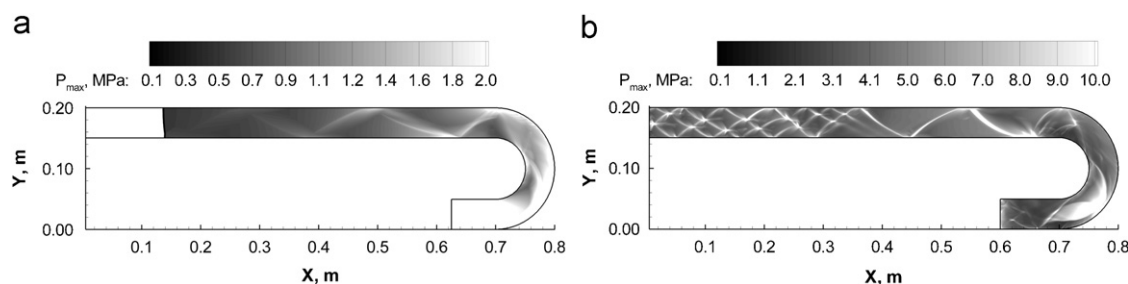


Fig. 11. Predicted maximal pressure field in the course of primary shock wave propagation in the tube with U-bend. Initial shock velocity is 1460 m/s; compression phase duration is 30  $\mu$ s (a) and 50  $\mu$ s (b). In the left figure, the shock wave decays, in the right figure the shock wave initiates detonation.

## 5. Concluding remarks

New experimental and computational results were obtained for shock and detonation transition through U-bends in curved tubes filled with a stoichiometric propane–air mixture. The experiments demonstrated a considerable effect of the U-bend on detonation initiation and propagation and supplemented the observations reported earlier for the U-bends of larger curvature radius.

On the one hand, the U-bend of the tube was shown to promote SDT considerably. Moreover, the tubes with the smaller curvature radius promoted SDT more efficiently than those with the larger curvature radius. Thus, it was proved experimentally that for the SDT in the tube with two U-bends of nearly limiting curvature, the velocity of the primary shock wave entering the first U-bend should exceed the value of about 800 m/s regardless the type of shock wave generator. In the tube with the larger curvature radius (Frolov, Aksenov, & Shamshin, 2005, 2007), the critical value of the primary shock wave velocity was at a level of 1100 m/s. Note also that direct detonation initiation in a straight tube of the same diameter required the primary shock wave propagating at a velocity exceeding 1700–1800 m/s.

On the other hand, the detonation wave propagating through the U-bend was shown to be subjected to temporary attenuation with a considerable velocity drop, followed by the recovery of the propagation velocity in the straight tube section downstream from the U-bend, or complete decay. The detonation decay was found to occur more likely in tubes with U-bends of a smaller curvature radius.

The computational studies revealed the important effect of compression phase duration in the primary shock wave on the SDT. The future work will be concentrated on

experimental studies of the U-tubes of other diameters and the development of the physical criteria describing the shock and detonation transition in terms of U-bend curvature, tube diameter, and shock wave compression phase duration.

## Acknowledgments

This work was partly supported by the US Office of Naval Research and International Science and Technology Center.

## References

- Frolov, S. M., Aksenov, V. S., & Basevich, V. Ya. (2005). Initiation of detonation in sprays of liquid fuel. *Advances in Chemical Physics*, 24(7), 71–79.
- Frolov, S. M., Aksenov, V. S., & Shamshin, I. O. (2005). Detonation propagation through U-bends. In G. Roy, S. Frolov, & A. Starik (Eds.), *Nonequilibrium processes. Combustion and detonation*, Vol. 1 (pp. 348–364). Moscow: Torus Press.
- Frolov, S. M., Aksenov, V. S., & Shamshin, I. O. (2007). Shock wave and detonation propagation through U-bend tubes. *Proceedings of the Combustion Institute*, 31, 2421–2428.
- Frolov, S. M., Basevich, V. Ya., & Aksenov, V. S. (2004). Combustion chamber with intermittent generation and amplification of propagating reactive shocks. In G. Roy, S. Frolov, & J. Shepherd (Eds.), *Application of detonation to propulsion* (pp. 240–249). Moscow: Torus Press.
- Frolov, S. M., Basevich, V. Ya., & Aksenov, V. S. (2005a). Optimization study of spray detonation initiation by electric discharges. *Shock Waves*, 14(3), 175–186.
- Frolov, S. M., Basevich, V. Ya., & Aksenov, V. S. (2005b). Decreasing the predetonation distance in a drop explosive mixture by combined means. *Doklady Physical Chemistry*, 401(Pt 1), 28–31.
- Nettleton, M. A. (1987). *Gaseous detonations*. London, New York: Chapman & Hall.
- Sturtevant, B., & Kulkarny, V. A. (1976). The focusing of weak shock waves. *Journal of Fluid Mechanics*, 73(4), 651–671.